22 July 1983, Volume 221, Number 4608 SCIENCE

High-Resolution Scanning Transmission Electron Microscopy

A. V. Crewe

Summary. The high-resolution scanning transmission electron microscope is being used in a growing number of laboratories. This article provides a general overview of the instrument and its capabilities for readers who are unfamiliar with it.

The idea of forming an image in an electron microscope by scanning the beam of electrons is almost as old as the electron microscope itself (*1*, *2*), and the very first images were based on the use of transmitted electrons. Little or no progress was made beyond this, however, because the technological requirements for this type of instrument are considerable and much of the technology was not available in the 1930's. In addition, the more familiar form of the electron microscope—the conventional transmission electron microscope (CTEM)—developed so rapidly and its resolving power became so good that it dominated the market.

It appears from the literature that these early ideas were largely forgotten, only to be revived again independently (*3*) when much of the technology for producing images by scanning techniques had become commonplace. The development of television, high-resolution display tubes, fast electronics, particle detectors, and high-vacuum systems provided almost all the necessary technology for the implementation of the concept.

The ideas for the construction of a high-resolution scanning transmission electron microscope (STEM) were put forward in 1963 (*3*). These ideas were based to a large extent on the techniques and practices of experimental work in nuclear physics and high-energy physics, with little or no regard for the vast amount of experience with the CTEM or, indeed, for the ideas for a secondary emission microscope (SEM) which were being pursued in Cambridge by Oatley (*4*) and his students. This has had both good and bad effects. On the one hand, cross-fertilization of this kind tends to bring in new ideas, but on the other hand the language can be very different and this can inhibit communication.

As one simple example of this kind of problem, in 1963 a thin specimen in a conventional electron microscope was considered as a weak phase object, while in the STEM we considered it to be a scattering object. As a consequence, the language associated with the conventional microscope was that of physical optics, where the effects of diffraction and interference play a dominant role, while that associated with the scanning microscope was concerned with scattering cross sections and angular distributions. Many other examples of this kind could be cited, but they all add up to a problem in communication. Virtually all these problems have now disappeared, and it is possible to use a common language. This progress was made possible by a recognition of the applicability of optical reciprocity (*5*) and careful analysis of the theoretical framework (*6*).

In nuclear physics and high-energy physics, one first needs a source of particles such as an accelerator. Accelerators are usually of sufficient complexity that their design and development constitute a separate subdiscipline of significant size. The interests of scientists working in this area are substantially confined to the region from the source of particles to the experimentalist's target. The accelerated beam of particles interacts with the target by elastic or inelastic collisions, and the detection and analysis of these events are in the province of the user of the accelerator.

The operating principles of the STEM bear more than a passing resemblance to those of accelerator physics. As shown in Fig. 1, an electron optic column is used to produce a well-defined beam of electrons. These electrons then pass through the specimen, where they undergo scattering by various processes. From the large number of possible processes, the user can select those of particular interest for examination. Images are made by scanning the incident beam in a raster and displaying the selected information as an intensity modulation of a magnified version of the raster.

Described in this way, we can obviously divide any discussion of the STEM into two distinct and separate areas—the probe-forming system and the detection system—since they are largely independent.

Probe-Forming System

The size and nature of the electron probe will largely determine the resolving power of the microscope, and for this reason considerable effort has been invested in understanding the limitations involved and in solving the many engineering problems. It was clear at the outset that a very small, very bright source of electrons was needed because the generation of an image by scanning means that all the image information from a point must be acquired in a much smaller time than in a conventional microscope. For this reason, field emission

A. V. Crewe is at the Enrico Fermi Institute and the Department of Physics and Biophysics, University of Chicago, Chicago, Illinois 60637.

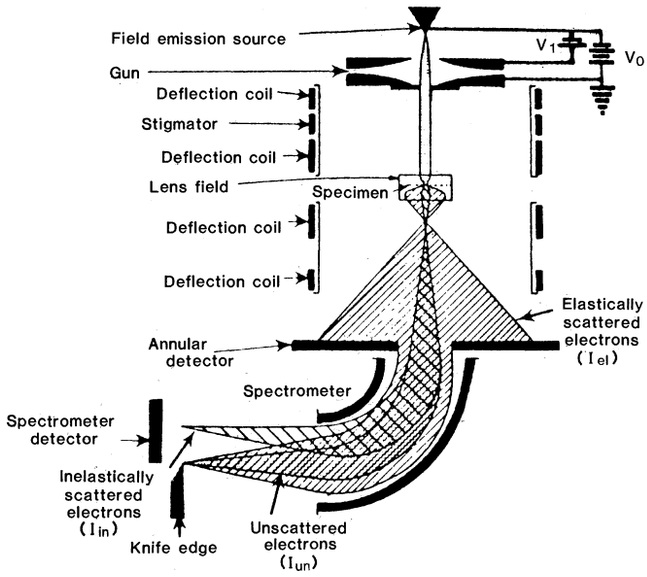

Fig. 1. Operational characteristics of the simplest STEM. Electrons from a field emission source are accelerated to a final potential V_0 and then focused on the specimen. Scattered electrons leaving the specimen are usually refocused by the magnetic field of the lens at some point farther down the column and then diverge. The elastically scattered electrons strike an annular detector, while the inelastic and unscattered electrons are separated by a spectrometer. The beam is scanned across the specimen by using deflection coils and below the specimen the scanning action is removed with additional deflection coils. The diagram is not to scale; for example, the maximum scattering angle for the electrons is in reality only 2° or 3°.

sources were developed (*7*), and it was later shown that they are the only sources available which have the properties required for the production of a diffraction-limited probe containing an electron current adequate for forming images (*8*).

Field emission sources usually operate with an applied potential of 2 or 3 kilovolts, and therefore the electrons must be accelerated further in order to provide them with enough energy to penetrate practical specimens (25 to 100 kV). Finally, magnetic lenses are used to produce the focused probe. The ultimate performance characteristics of an STEM are determined by the nature of this probe. Its physical dimensions and the electron beam current are set by the total spherical aberration of the lenses, diffraction, and the size and brightness of the source.

There are some aspects of the probe-forming column which are perhaps not universally appreciated and which considerably simplify the analysis and understanding of this system. It can be shown (*8*) that the probe current in a diffraction-limited probe at any voltage is given by

$$I_p = \text{constant} \times \beta \left(\frac{\delta_s}{\delta_0}\right)^2$$

where β is the brightness of the source and δ_s/δ_0 is the ratio of the real image of the source to the diffraction-limited image ($0.61\lambda/\alpha$). The quantity δ_s/δ_0 can be most easily defined in the source region itself by only allowing a small portion of the total emission current to pass through an aperture and down the column. For a thermionic source of electrons, β has a value of about 2 (amperes per square centimeter per steradian per volt); for a LaB_6 source β is in the range 10 to 100; and for a field emission source β is in the range 10^3 to 10^4. The use of such a high value of β allows us to reduce the value of (δ_s/δ_0) to the point where $\delta_s \ll \delta_0$.

We can now turn the argument around to say that if there are no further physical apertures in the column the total probe current, I_p, is a constant of the system, and then δ_s/δ_0 is defined for any focus anywhere in the column. In other words, any probe that is formed will be diffraction-limited and the Gaussian image of the source will always remain in the same ratio δ_s/δ_0.

The ability to define the probe current at the source itself makes the calculation of the beam current a trivial problem; the corollary is that, to a large extent, the quality of the final image is substantially defined.

As is the case with conventional microscopes, the ultimate resolving power is limited mainly by the spherical aberration of the entire column. With proper design this is usually determined by the final (objective) lens. Classically, the effect of this spherical aberration can be reduced by using a small angle of convergence of the electron beam, but we must also consider diffraction effects and defocus. The problem of optimizing these effects was examined by Black and Linfoot (*9*), who showed that for a lens with a given amount of spherical aberration there is an optimum focus close to but not coincident with the Gaussian (paraxial) focus and there is an optimum aperture that should be used. This aperture is defined by the convergence angle of the beam, which should be

$$\alpha_0 = \left(\frac{4\lambda}{C_s}\right)^{1/4}$$

and the position of the optimum focus is at a defocus value of $\Delta f = -(\lambda C_s)^{1/2}$. The results of Black and Linfoot can be expressed in two ways: (i) by the equivalent of the Rayleigh limit, which is then given by

$$\delta_0 = 0.43 C_s^{1/4} \lambda^{3/4}$$

where C_s is the coefficient of spherical aberration, or (ii), more completely, by the optical transfer function (OTF), which is the Fourier transform of the intensity distribution in the focused probe. The OTF then gives the response of the system to the various spatial frequencies of a specimen. It is shown in Fig. 2, which clearly indicates the absence of any zeros or oscillations and shows that it has a shape entirely equivalent to the OTF of a camera. The absence of zeros and oscillations in the OTF is one of the distinguishing features of the STEM.

The expression for δ_0 given above can be converted into numbers by choosing a lens $C_s \sim 0.04$ cm so that at 30 kV or so the resolution is 2.4 Å. These are the parameters of our system, and other microscopes operate at a similar resolution since this represents something close to a practical limit.

It seems clear from this description that the STEM has many attractive features which can, in principle, simplify the acquisition and interpretation of images. In spite of this, the STEM is not yet a popular instrument. Field emission sources require an ultrahigh-vacuum system (10^{-10} torr), which is both more expensive and more difficult to operate than a diffusion-pumped system. One benefit of using such a system, however, is that the necessity for periodic cleaning of the column is eliminated. It must be clean in the first place if it is to operate at all, and there is no source of contamination to make it dirty. Some such systems now in operation have not been cleaned or opened at all for years.

The use of field emission sources and ultrahigh-vacuum systems has undoubtedly inhibited acceptance of the STEM; conventional hot-filament sources are much easier to use and understand, and conventional vacuum systems are easier to operate. In addition, the early attempts to use field emission sources were not always successful, since the field emitting tips had an unfortunate

tendency toward self-destruction. Most, if not all, of these difficulties have now been overcome, however, and source lifetimes of several years are not uncommon. Automatic tip management systems are now incorporated into some microscopes so that the operator is unaware of the nature of the source. These and other improvements should eventually remove the remaining concerns about reliability.

Postspecimen Optics and Detectors

As with accelerator physics, the kind and complexity of the optical system following the specimen depend on the information required and the difficulty in acquiring it. Our system is one of the simplest and consequently is somewhat limited in flexibility.

The electrons that emerge from the specimen can be thought of as being in one of three groups: unscattered, elastically scattered, and inelastically scattered. The elastically scattered electrons are scattered through large angles and are approximately proportional in number to $Z^{3/2}$, where Z is the atomic number of the scattering element. The inelastically scattered electrons are scattered through small angles and their number is roughly proportional to $Z^{1/2}$. This distinction in space and Z dependence can be put to use in several ways. The mean scattering angle of elastically scattered electrons is large, so that they can be detected or counted with very high efficiency (90 percent or more) by using a detector in the shape of an annulus, while the small scattering angle for inelastic electrons allows them to be separated from the unscattered electrons with a simple spectrometer, also with high efficiency (see Fig. 1).

This simple system allows us to obtain two types of information simultaneously point by point in the specimen, one proportional to $nZ^{3/2}$, where n is the number of atoms in the probe, and one proportional to $nZ^{1/2}$. It is then possible to determine approximate values for Z and n from these values to estimate a molecular weight. The ability to perform such measurements is one of the principal advantages of the STEM (*10*).

The high efficiency of collection of elastically scattered electrons provides an electrical signal with a good signal-to-noise ratio, and the use of an annular detector (Fig. 1) means that this is a dark-field signal so that the background is low. As a consequence of this and the high resolution, single atoms of medium to high Z are readily visible even when supported by a thin carbon film (Figs. 3 to 6). The ease with which this can be accomplished and the clarity of the images are other distinguishing features of the STEM.

This simple detector arrangement is adequate for the tasks mentioned above, namely separating the inelastic and elastic signals for further processing and dark-field observations of small objects.

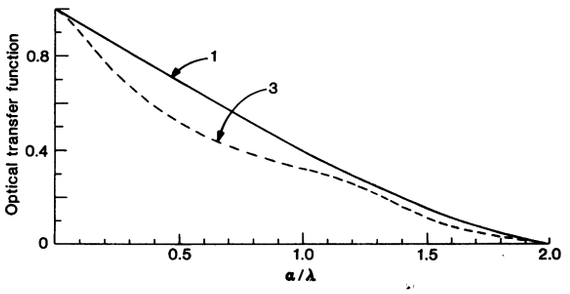

Fig. 2. Optical transfer function versus α/λ. The OTF indicates the ability of an optical device to transmit the various spatial frequencies of the image information. This frequency is given in units of α/λ, where α is the semiangle of convergence at the focus and λ is the wavelength. Curve 1 shows the OTF of a perfect lens and is that obtained, for example, with a very expensive camera. Curve 3 shows the OTF of a STEM when operated under optimum conditions. The difference between the two curves is due to the finite spherical aberration of the lenses.

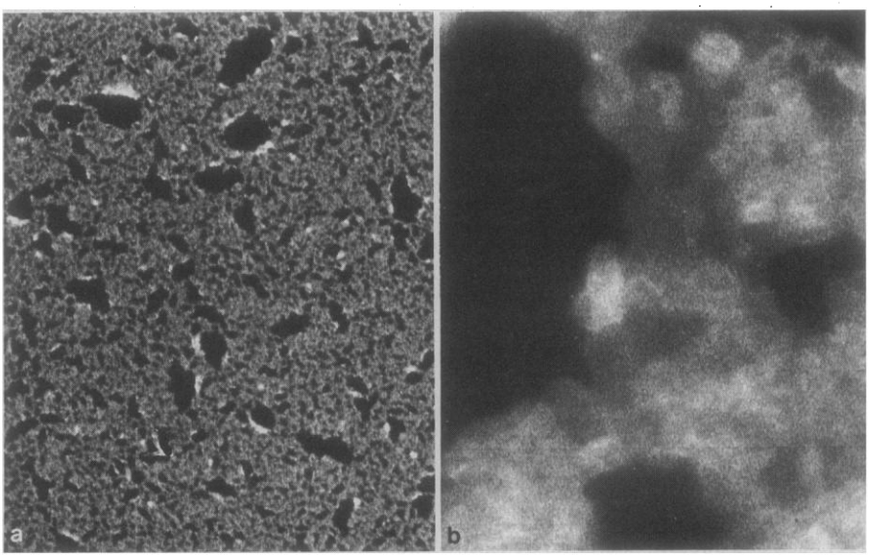

Fig. 3. A thin film of carbon, one of the most suitable substrates for biological specimens. This particular film is very thin (average ~ 7 Å). (a) Low-magnification view (full scale, 1000 Å) and (b) high-magnification view (full scale, 100 Å). The latter indicates the existence of discrete steps in thickness corresponding to 1, 2, 3, . . . atom layers. [Micrograph by M. Ohtsuki]

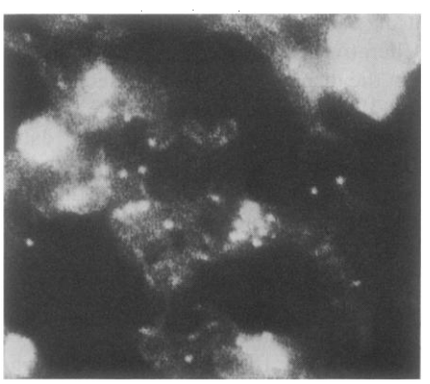

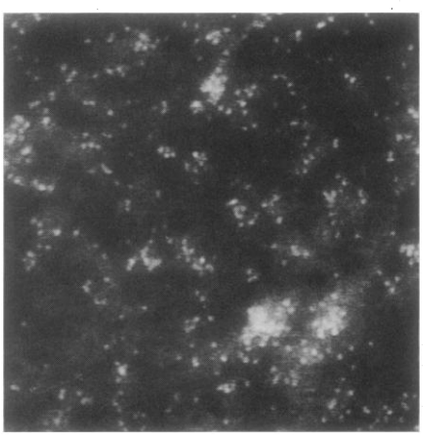

Fig. 4 (left). Micrograph in which atoms of gold can be seen. A drop of a dilute solution of gold chloride was allowed to dry on a substrate similar to that in Fig. 3. Small clusters and single atoms of gold are readily visible (full scale, 70 Å). Fig. 5 (right). Preparation similar to that in Fig. 4 except that the material used was uranyl acetate. Uranium atoms and some clusters are readily visible (full scale, 200 Å). [Micrograph by M. Ohtsuki]

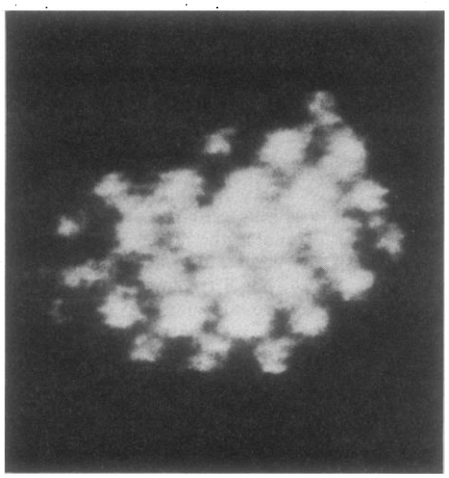

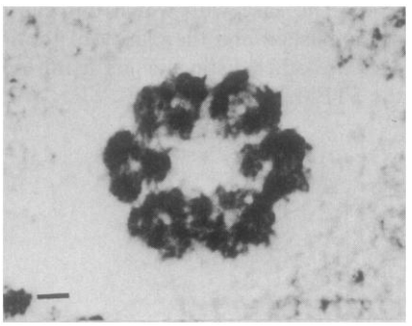

Fig. 6 (left). STEM micrograph of a small crystal of UO_2 formed by decomposition of uranyl acetate in the electron beam. The full-scale horizontal dimension is 35 Å, and the crystal structure is clearly visible. The lighter spots are single atoms, and the brighter spots in the center are presumably due to the superposition of several atoms that are accidentally aligned with the beam. [Micrograph by M. Ohtsuki] Fig. 7 (right). STEM micrograph of the giant hemoglobin of *Lumbricus terrestris* (common earthworm). The hemoglobin was stained with 1 percent uranyl acetate. This micrograph was obtained by using optimal scanning near the Nyquist rate and the scan line structure was removed by optical filtration. The remaining background line structure, which is faintly visible, is due to small variations in the scan line spacing. Scale bar, 50 Å; electron dose, 10 to 20 electrons per square angstrom. [Micrograph by M. Ohtsuki]

It is inadequate, however, for the acquisition of more sophisticated data. Diffraction information is, of course, of great importance, and while one can observe diffraction contrast with this arrangement, it is difficult to display a good diffraction pattern since a very small aperture must be used and the incident beam current must be considerably higher than that used in a conventional microscope. This situation can be corrected by using more optical elements, the most complicated and flexible being one proposed and put into operation by Cowley and Spence (*11*). It seems highly likely that new optical systems will continue to be developed for the solution of other measurement problems, and in this respect the STEM offers more flexibility than a conventional microscope because the probe-forming system is largely unaffected.

Display System

The pictorial information is obtained as electrical signals from the various detectors and appears sequentially as the microscope beam is scanned across the specimen. In view of this, it would seem to be a simple matter to display this information as as intensity modulation of an oscilloscope. There are, however, some problems here which have also inhibited general acceptance of the instrument.

It is possible, in principle, to scan at TV rates and display an image on a TV screen. However, this would require higher beam currents than are normally available, and in any case the specimen damage would be too high. Finally, the quality of a TV image is not very great since the number of identifiable picture elements (pixels) is too small.

The other method is that normally employed in an STEM. This involves using a slow scan and a long-persistence phosphor on the oscilloscope. The slow scan makes focusing difficult and time-consuming, but it is possible to obtain an image of 1024 by 1024 pixels provided a high-quality display tube is used. The only major criticism of this approach is that the visible output is not well matched to human physiological responses.

This situation can be improved by using some form of scan converter whereby the microscope scans slowly but the display screen is scanned quickly at TV rates. This requires some form of analog or digital memory for the data. Digital memories are becoming less expensive daily, and it seems clear that this will be the preferred approach in the future. A 1024 by 1024, 8 bit per pixel memory and display tube can be acquired at a reasonable cost and is compatible with full-color displays.

Even such a large memory and high-resolution display cannot compare with the piece of film that is used in a CTEM. Images of 5000 by 5000 pixels can easily be contained on film. The STEM cannot match this performance, and the microscopist who is accustomed to selecting a small piece of film for subsequent enlargement will be disappointed. On the other hand, it is relatively simple to take several hundred images per day with the STEM, store them on magnetic tape, and replay them at high speed for selection of the relevant ones.

Electron Energy Loss

For the very simple detection system described above, we need some form of electron energy loss spectrometer in order to separate the inelastically scattered electrons from electrons that have undergone no scattering at all. It is then convenient to use the spectrometer to extract more detailed information about the specimen point by point.

Energy loss spectroscopy is a subject of wide interest and considerable activity and can only be briefly summarized here. A more complete discussion of some of these topics can be found in the article by Joy and Maher (*12*). It is only in recent years that this form of specimen analysis has been combined with the high spatial resolution capabilities of the STEM on a regular basis, but the principles were, in fact, incorporated from the beginning (*3*).

The information available in the spectrum of energy losses is considerable. In the energy loss region from 0 to 10 electron volts the spectrum that is observed can be related mathematically to the optical absorption spectrum, although the resolution is usually considerably worse. In the region 10 to 50 eV the spectrum is usually featureless, consisting of a broad maximum at 20 to 25 eV, the so-called plasma loss exhibited by most solids. Exceptions do occur, most notably for aluminum, which has a well-defined and sharp plasma loss at 15 eV with multiples at 30 eV, 45 eV, and so on.

Specific elemental information can be obtained with losses equal to or greater than the x-ray excitation energies. For the *K* shell these "edges" are very well defined and easily obtained. For the *L* and *M* shells the edges are usually more difficult to locate because they occur on the trailing edge of the broad plasma loss, which is usually considerably broadened by multiple scattering and consequently multiple losses. On the other hand, the collecting power of the spectrometer is generally much higher for the *L* and *M* than for the *K* losses, so that they are often the preferred ones to use. It would be highly desirable to be able to use these x-ray edges as a quan-

titative tool for the elemental analysis of unknown specimens, but the complications that arise from multiple scattering and spectrometer acceptance angle make this difficult. Recent developments in theory (*13*) and spectrometer design (*14, 15*) may very well make this possible.

The leading edge of the x-ray loss lines also contains chemical information since the binding energy of the atom must be taken into account. This inclusion means that the precise position of the leading edge of the line is subject to "chemical shift" and several peaks are often seen superimposed (*16*).

The trailing edge of the x-ray loss lines contains information about the spacing between atoms of the particular element in the specimen. This EXELFS (extended x-ray energy loss spectrum) region shows small oscillations of intensity due to the inhibition of emission of ejected electrons in particular directions in a crystal at particular energies, and a Fourier transform of the spectrum can provide nearest-neighbor distances.

Finally, most if not all of these energy loss spectra can be expected to depend on the direction of emission with respect to crystal orientation or other regular structural features. This feature has only recently begun to be explored and promises to be of considerable importance [see, for example (*17*)].

It is usually true that as we try to extract more detailed information from a system we lose intensity, and this is particularly the case for electron energy loss. This in turn means that we must use a large electron current and must necessarily incur specimen damage. Several techniques are coming into use which could help to alleviate this problem. For example, we could use many detectors in parallel to acquire the spectral information or we can try to improve the collecting power of the spectrometer (*14, 15*), or both. This is an active area of research, and we can expect significant improvements in the future.

One other limitation is a fundamental one. For an energy loss ΔE the mean scattering angle is of the order of $\Delta E/E$, which may be quite small, and according to the uncertainty principle the "impact parameter" is proportional to the inverse of this angle. This means that for small energy losses the energy loss events are not well localized and this information cannot be used at high resolution. For example, we observed a loss of resolution to about 10 Å with energy loss electrons where $\Delta E \sim 20$ volts. For *K*-shell losses this is not a problem, and the spatial resolution can be as high as the probe-forming optics permit.

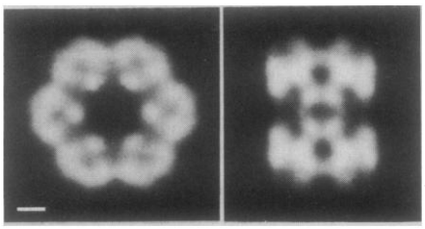

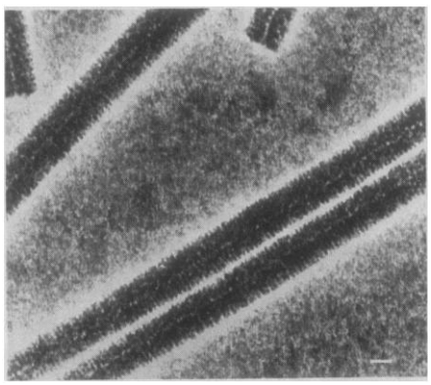

Fig. 8 (left). Additional micrographs of the giant hemoglobin of *Lumbricus terrestris* (see Fig. 7), showing the side and top views (scale bar, 50 Å). Each represents the sum of several separate images of distinct molecules, 36 for the top view and 50 for the side view. The images were summed and averaged by digital methods. The specimen was negatively stained with uranyl acetate. Electron dose, 1 to 2 electrons per square angstrom. [Micrograph by M. Ohtsuki] Fig. 9 (right). STEM micrograph of tobacco mosaic virus. The image was obtained with the annular detector and therefore represents elastically scattered electrons. The virus was stained with 1 percent uranyl acetate. Some structure from the scan system can be seen in the image. This can be removed optically if necessary (see Fig. 7). Scale bar, 100 Å; electron dose, 11 electrons per square angstrom. [Micrograph by M. Ohtsuki]

In summary, inclusion of an energy loss spectrometer in the STEM offers a wealth of opportunities for the analysis of specimens and, together with a good spatial resolution, this promises to open several new avenues of approach to analysis at or near the atomic level.

Image Processing

The image format of the STEM is naturally adapted to digital image processing techniques. The image is constructed in serial form, point by point and line by line. Thus it can be readily digitized and stored in a computer memory. In this respect there is another advantage. The electron probe in a diffraction-limited STEM is band-limited, and the OTF has a definite upper limit of $2\lambda/\alpha$. This means that it is possible to scan at the Nyquist rate and avoid aliasing problems, or, to put it another way, the image can be constructed with the lowest possible number of digitized points (Fig. 7). This is much more difficult to accomplish when the digitization is done by optically scanning an image obtained in a conventional microscope. In this case one must use overscan methods and consequently process more than the minimum amount of data.

Digital signal processing is of particular interest in high-resolution microscopy of biological objects. It is by now well known that such materials are susceptible to radiation damage by the electron beam. This damage can span the range from loss of high-resolution diffraction data to complete destruction. It is generally accepted that a specimen dose in the range 1 to 2 electrons per square angstrom or less is needed if one is to retain high-resolution information. The classical work of Unwin and Henderson (*18*) on the purple membrane was done with doses in this range.

Such low doses necessarily give images with a great deal of statistical noise, and the only way to obtain detailed information is to average over many identical objects. Unwin and Henderson were able to perform such an average by using a two-dimensional crystal; but in many cases such a configuration cannot be produced. The other approach is to average over many identical objects by summing separate images. Many examples of this can be found in the work of Frank and co-workers (*19*), again done with a conventional microscope.

This method is the most appropriate one for the STEM and is the one we have used. It works particularly well with dark-field elastically scattered electrons because of the high collection efficiency. Even with such low doses the images are visible and interpretable, which makes summation possible without the need for cross-correlation techniques to locate the objects of interest. The image of a single hemoglobin molecule shown in Fig. 7 was obtained by scanning at the Nyquist rate with subsequent optical filtration. The image in Fig. 8 was obtained by summing many digitized images of different molecules with subsequent digital processing. The image in Fig. 9 was also scanned at the Nyquist rate and is shown in its original form without subsequent optical filtration.

Another interesting aspect of digital processing which could be applied to

either type of microscope is false color conversion. The human eye has severe limitations when viewing an image in monochrome, 12 to 16 levels of intensity being about the maximum that can be distinguished at any one time. This is incompatible with the microscope imaging process, where several hundred statistically meaningful intensity levels may be present. False color conversion offers the opportunity to present to the eye the entire information content of an image. We have developed a system that allows 32 colors and are expanding it to 256 colors (*20*). What will be needed eventually is a standard color conversion algorithm that has a universal meaning and can be interpreted by anyone.

Our work on the use of false color has indicated that it can be of significant value in some circumstances, but can also produce confusing images. If the image has high statistical quality and the objects of interest are well separated physically, the use of color is a definite advantage. Subtle shadings of intensity that are invisible in monochrome become very clear in color, and instant judgments can be made on such factors as specimen thickness and quality of staining. On the other hand, a statistically noisy image is much more easily interpreted in monochrome. The eye can average the noise easily, but in color one cannot average neighboring colors quite so easily. Similarly, overlapping objects can be seen and interpreted as such in monochrome, but in color the result is confusion and total inability to interpret the overlapping region. It is very convenient to have both systems in operation simultaneously to allow the operator to fully appreciate the images.

Future Prospects

The collection efficiency of elastically scattered electrons for dark-field contrast is so close to the theoretical limit that no further advances can be expected. This is not true, however, for the collection efficiency of inelastically scattered electrons. A spectrometer that combines high momentum resolution and high enough collection efficiency is not yet available. Such a spectrometer would be of great value, but its development awaits ideas for the complete correction of its many aberrations, all of which either degrade resolution or lower efficiency or both. The ability to collect all such electrons and simultaneously measure their energy would provide an extra dimension of image detail. It is even conceivable that such a system could succeed in identifying single atoms by their x-ray absorption characteristics.

As pointed out above, more sophisticated detection systems are possible—for example, by combining energy analysis with diffraction information. It is not difficult to imagine special schemes for detection aimed at the extraction of particular data, and one might expect many systems of this kind to be developed.

Spatial resolution will continue to receive attention. Both the STEM and the CTEM have reached practical limits. The value of C_s is primarily determined by the focal length of the lenses that are used, and these have practical limits imposed by the maximum magnetic field strength and the need for accessibility for the insertion and manipulation of specimens. It might be argued that higher resolution is possible if we reduce λ by increasing the accelerating voltage. Here again, however, practical limits occur, particularly in the precise regulation of these very high voltages.

We cannot anticipate the development of lenses with significantly lower values of C_s. Scherzer's theorem (*21*) and almost 50 years of experience support this notion. However, correction of C_s by an additional optical element appears to be possible in principle. Scherzer proposed such a system in 1946 (*22*) and recent results give reason to hope that this scheme may work (*23*).

In its simplest form, this system would have four quadrupole and three octupole lenses, for a total of 40 pole pieces, and the mechanical tolerances are very severe ($\sim \pm 0.1$ micrometer). This means that it is enormously difficult to align and to maintain this alignment. Our attempts to make such a system work failed (*24*), and it is a tribute to the skill of the group in Darmstadt that they have had even partial success.

Recently, we proposed another method of correction involving two sextupoles, for a total of 12 pole pieces, and there is reason to believe that this simpler system could be made to work (*25*). Beck (*26*) also proposed a system with sextupoles, which operates on different principles.

On the supposition that one or other of these schemes will be successful, one can ask what the next limitation would be. We have investigated this point (*27*) and conclude that for a conventional electron source the resolution would be limited first by the energy spread of the electrons. (In this respect, it should be noted that the Scherzer corrector incorporates chromatic correction.) With a field emission source this effect can be made small since the energy spread itself is small, and in this case the next limit would be the combined effects of fifth-order aperture aberration, diffraction, and defocus. In an optimal system a resolving power in the neighborhood of 0.5 Å appears possible. In other words, the effects of correcting C_s would be a gain of a factor of 4 or 5 in resolution.

Such a factor would be of considerable significance in materials research. The present resolution of 2 to 2.5 Å is insufficient to resolve distances between atoms in most solids, although a variety of means have been used to circumvent this problem in special cases. A point resolution of 0.5 Å would allow one to obtain images that would resolve such distances in most solids. In view of all these recent developments, such a goal no longer seems impossible.

References and Notes

1. M. V. Ardenne, *Naturwissenschaften* **19**, 407 (1938).
2. W. Knecht, *Ann. Phys. (Leipzig)* **20**, 161 (1934).
3. A. V. Crewe, *J. Microsc.* **2**, 369 (1963).
4. C. W. Oatley, *J. Appl. Phys.* **53** (No. 2), R1 (1982).
5. H. V. Helmholtz, *Grelles J.* **100**, 213 (1886).
6. E. Zeitler and M. G. R. Thompson, *Optik* **31**, 258 (1970).
7. A. V. Crewe and J. Wall, *J. Mol. Biol.* **48**, 375 (1970).
8. A. V. Crewe, *Rep. Prog. Phys.* **43**, 621 (1980).
9. G. Black and E. H. Linfoot, *Proc. R. Soc. London Ser. A* **239**, 522 (1957).
10. J. Wall, thesis, University of Chicago (1971).
11. J. M. Cowley and J. C. H. Spence, *Ultramicroscopy* **3**, 433 (1979).
12. D. C. Joy and D. M. Maher, *Science* **206**, 162 (1979).
13. J. C. H. Spence, *Ultramicroscopy* **4**, 9 (1979).
14. O. L. Krivanek and P. R. Swann, in *Quantitative Microanalysis with High Spatial Resolution* (Metals Society, London, 1981), p. 136.
15. F. Scaduto, private communication.
16. M. S. Isaacson, *J. Chem. Phys.* **56**, 1813 (1972).
17. M. M. Disko, O. L. Krivanek, P. Rez, *Phys. Rev. B* **25**, 4252 (1982).
18. P. N. T. Unwin and R. Henderson, *J. Mol. Biol.* **94**, 425 (1975).
19. J. Frank, W. Goldfarb, D. Eisenberg, T. S. Baker, *Ultramicroscopy* **3**, 283 (1978).
20. A. V. Crewe and M. Ohtsuki, *ibid.* **9**, 101 (1982).
21. O. Scherzer, *Z. Phys.* **101**, 593 (1936).
22. ———, *Optik* **2**, 114 (1947).
23. H. Hely, *ibid.* **60**, 353 (1982).
24. V. Beck, *Proc. 35th Annu. Meet. Electron Microsc. Soc. Am.* (1977), p. 30.
25. A. V. Crewe, *Optik* **60**, 271 (1982).
26. V. Beck, *ibid.* **53**, 237 (1979).
27. A. V. Crewe and D. Salzman, *Ultramicroscopy* **9**, 373 (1982).

28. Supported by a grant from the U.S. Department of Energy. I would like to acknowledge the help given by Mitsuo Ohtsuki, who provided these micrographs and whose skills are made evident by their high quality. In addition, the advice of the reviewers has been of great help and has improved the accuracy and readability of the article.